



## Article

# Modelling Species Richness and Functional Diversity in Tropical Dry Forests Using Multispectral Remotely Sensed and Topographic Data

Víctor Alexis Peña-Lara <sup>1</sup>, Juan Manuel Dupuy <sup>1</sup> , Casandra Reyes-García <sup>1</sup> , Lucía Sanaphre-Villanueva <sup>2</sup> , Carlos A. Portillo-Quintero <sup>3</sup> and José Luis Hernández-Stefanoni <sup>1,\*</sup>

<sup>1</sup> Centro de Investigación Científica de Yucatán A.C., Unidad de Recursos Naturales, Calle 43 #130, Colonia Chuburná de Hidalgo, Mérida C.P. 97200, Yucatán, Mexico

<sup>2</sup> Centro del Cambio Global y la Sustentabilidad A.C., Consejo Nacional de Ciencia y Tecnología, Calle Centenario del Instituto Juárez S/N Col. Reforma, Villahermosa C.P. 86080, Tabasco, Mexico

<sup>3</sup> Geospatial Technologies Laboratory, Department of Natural Resources Management, Texas Tech University, Box 42125, Lubbock, TX 79409-2125, USA

\* Correspondence: jl\_stefanoni@cicy.mx; Tel.: +52-999-942-8330 (ext. 366)

**Abstract:** Efforts to assess and understand changes in plant diversity and ecosystem functioning focus on the analysis of taxonomic diversity. However, the resilience of ecosystems depends not only on species richness but also on the functions (responses and effects) of species within communities and ecosystems. Therefore, a functional approach is required to estimate functional diversity through functional traits and to model its changes in space and time. This study aims to: (i) assess the accuracy of estimates of species richness and tree functional richness obtained from field data and Sentinel-2 imagery in tropical dry forests of the Yucatan Peninsula; (ii) map and analyze the relationships between these two variables. We calculated species richness and functional richness (from six functional traits) of trees from 87 plots of the National Forest Inventory in a semi-deciduous tropical forest and 107 in a semi-evergreen tropical forest. Species richness and functional richness were mapped using reflectance values, vegetation indices, and texture measurements from Sentinel-2 imagery as explanatory variables. Validation of the models to map these two variables yielded a coefficient of determination ( $R^2$ ) of 0.43 and 0.50, and a mean squared relative error of 25.4% and 48.8%, for tree species richness and functional richness, respectively. For both response variables, the most important explanatory variables were Sentinel-2 texture measurements and spectral bands. Tree species richness and functional richness were positively correlated in both forest types. Bivariate maps showed that 44.9% and 26.5% of the forests studied had high species richness and functional richness values. Our findings highlight the importance of integrating field data and remotely sensed variables for estimating tree species richness and functional richness. In addition, the combination of species richness and functional richness maps presented here is potentially valuable for planning, conservation, and restoration strategies by identifying areas that maximize ecosystem service provisioning, carbon storage, and biodiversity conservation.

**Keywords:** plant diversity; functional diversity; functional traits; Sentinel-2; texture analysis; national forest inventory



**Citation:** Peña-Lara, V.A.; Dupuy, J.M.; Reyes-García, C.; Sanaphre-Villanueva, L.; Portillo-Quintero, C.A.; Hernández-Stefanoni, J.L. Modelling Species Richness and Functional Diversity in Tropical Dry Forests Using Multispectral Remotely Sensed and Topographic Data. *Remote Sens.* **2022**, *14*, 5919. <https://doi.org/10.3390/rs14235919>

Academic Editor: Michael Vohland

Received: 26 October 2022

Accepted: 21 November 2022

Published: 23 November 2022

**Publisher's Note:** MDPI stays neutral with regard to jurisdictional claims in published maps and institutional affiliations.



**Copyright:** © 2022 by the authors. Licensee MDPI, Basel, Switzerland. This article is an open access article distributed under the terms and conditions of the Creative Commons Attribution (CC BY) license (<https://creativecommons.org/licenses/by/4.0/>).

## 1. Introduction

Tropical dry forests (TDF) experienced a sharp decline in plant cover and biodiversity associated with land-use changes and climate change [1,2]. Together, these stressors and the poor protection of TDF seriously threaten their sustainability, biodiversity, and the ecosystem services they provide [3]. Thus, information on the spatial distribution of vegetation attributes such as diversity is essential for diagnosis and continued monitoring

to adopt appropriate local or regional measures for biodiversity conservation and promote suitable ecosystem management strategies.

Efforts to assess and understand changes in plant biodiversity focused on the analysis of taxonomic diversity [4], mainly through species richness (the number of species per area sampled). However, the resilience of ecosystems (including their diversity) depends not only on species richness but also on the functions of species within ecosystems, including their environmental tolerances and ecological requirements, as well as their effects on ecosystem functioning [5,6]. Thus, in recent decades there was a growing interest in assessing not only taxonomic diversity but also functional diversity (FD) [7,8].

FD is defined as the range, abundance, and relative distribution of the functional traits of organisms in a community [6]. In other words, FD refers to the variation of functional traits between organisms that influence individual fitness and ecosystem functioning [9]. Functional traits are biological (physiological, morphological, anatomical, biochemical, or behavioral) characteristics measurable at the individual level that affect the growth, reproduction, or survival of a species [10]. Some of the most commonly used functional traits of plants are maximum height, wood density (dry weight divided by fresh volume), leaf habit (deciduous vs. evergreen species), leaf area (leaf surface), specific leaf area (leaf surface divided by dry weight), and leaf dry matter content (dry weight divided by fresh weight) [11].

There are several FD indices. One of the most widely used is functional richness (FRic), which allows for the analysis of the mechanisms linking biodiversity to ecosystem functioning by providing information on the distribution of species according to functional traits [12,13]. Particularly, FRic was related to two mechanisms of community assembling: environmental filtering and niche differentiation [14]. In addition, it was demonstrated that FRic is significantly correlated with ecosystem functioning [15,16] and with net and gross primary productivity [17]. The latter is the largest flow component of the global carbon cycle [18].

Remote sensing data were successfully used to predict species richness in large areas of different ecosystems [19] on global [20,21], regional [22], or local [23] scales. These data include reflectance values and vegetation indices calculated from the spectral bands of satellite imagery. Species diversity was found to be negatively related to the red band and positively to the infrared band due to chlorophyll absorption and light scattering in the leaf [24]. In addition, vegetation indices are positively related to species diversity, given the relationship between species diversity and productivity [25]. However, habitat heterogeneity, measured as spectral variability, is considered one of the most important factors for predicting species diversity since areas with greater environmental variation are associated with a higher number of both ecological niches and species [26]. Spectral variability can be estimated through different approaches. We used texture measures as a proxy for spectral variability because these measures reflect the spatial variation within an image [27].

Functional richness was estimated by the relationship between field-measured FD and abiotic factors such as climate and soil. However, this approach is limited by the coarse resolution of abiotic factor data [28]. On the other hand, the functional traits of plants influence their ability to absorb or reflect sunlight so that these traits can be detected from optical images [29]. Most studies predicting functional richness were performed using hyperspectral images, characterized by very high spatial resolution, strengthened by hundreds of spectral bands capable of measuring reflectance throughout the entire electromagnetic spectrum [17,30–32]. Although data from these sensors demonstrated good predictive power for estimating FD, they are not available for extensive areas, so their use for vegetation monitoring and ecosystem evaluation is limited [33]. Consequently, most studies on functional diversity were conducted in small areas [33]. To estimate functional richness over large areas, new studies used sensors with a spatial resolution between 10 m and 30 m, such as Landsat [34] and Sentinel-2 [8,33]. However, no studies of this kind were conducted in tropical dry forests.

A major limitation for estimating FD with Landsat or Sentinel-2 sensors is pixel size since several individuals of different species can be found in areas of 100 m<sup>2</sup> to 900 m<sup>2</sup> [19], while field data for functional traits are based on individuals. This study used data on functional traits from individual trees to calculate the mean community-weighted functional trait. Although Sentinel-2 images do not have as many bands as hyperspectral images, some studies suggested that good estimates of functional traits can be obtained with Sentinel-2 bands [8,33]. Besides, differences between the distribution of plants in forests can be detected with texture metrics, identifying the vertical forest structure [35]. Therefore, spectral heterogeneity was also positively related to functional richness and productivity in forest communities [7]. Consequently, the use of texture metrics can help improve the accuracy of estimates of species richness and functional richness in plant communities.

Several studies documented a positive relationship between various functional diversity components and plant species richness [36–38]. However, tropical dry forests show no clear evidence of the association between plant species richness and functional richness since most of these studies addressed other forest types. Elucidating the type of association is hugely important as it can support the most appropriate strategies for mitigating biodiversity loss and conserving terrestrial ecosystems. The reason is that areas with higher plant species richness and higher functional richness can ensure a greater provision of ecosystem services to society; this contributes to mitigating global climate change through atmospheric carbon uptake and storage while mitigating plant biodiversity loss. It also provides relevant information for decision-making as it would help identify key areas for conservation, restoration, and protection.

This study aimed to assess the accuracy of species richness and functional richness estimates obtained from high-resolution Sentinel-2 imagery and field data in the tropical dry forests of the Yucatan Peninsula. Due to the documented saturation of vegetation indices under dense canopy conditions, particularly in tropical forests [19], the use of spectral texture metrics is expected to provide a more accurate prediction of plant species richness and functional richness. In addition, spatial relationships between plant species richness and functional richness were assessed through bivariate maps in the two forest types studied.

## 2. Materials and Methods

### 2.1. Study Area

The study area comprises two types of tropical dry forests in the Yucatan Peninsula (Figure 1). The area was selected in order to have greater variability in vegetation and its attributes (taxonomic and functional richness) and obtain greater representativeness of the maps generated from remote sensing data. Both sites have an area of 3600 km<sup>2</sup>. The first site (Kaxil Kiuic) is located in the south of the state of Yucatan (20°04′–20°06′N, 89°32′–89°34′W) and is covered by a tropical semi-deciduous forest [39] in which about 50% to 75% of the trees shed their leaves during the dry season [39]. The dominant species are *Neomillspaughia emarginata*, *Gymnopodium floribundum*, *Bursera simaruba*, *Piscidia piscipula* and *Lysiloma latisiliquum*. Mean annual precipitation ranges between 900 mm and 1100 mm [40], and the local geomorphology combines flat areas with limestone hills of moderate slopes. The landscape consists mainly of forest land (94% of the area), mostly dominated by forest stands of different successional ages [41]. The second site (Felipe Carrillo Puerto) is located in the southwest of Yucatan. This site is relatively flat, with mean annual precipitation ranging from 1100 mm to 1300 mm. The dominant vegetation is the tropical semi-evergreen forest, where only 25% to 30% of the species shed their leaves during the dry season [39]. The most abundant species are *Manilkara zapota*, *Vitex gaumeri*, *Bursera simaruba*, *Metopium brownei* and *Cecropia obtusifolia*. The landscape is composed of a mosaic of agricultural fields and patches of forests of different successional ages.

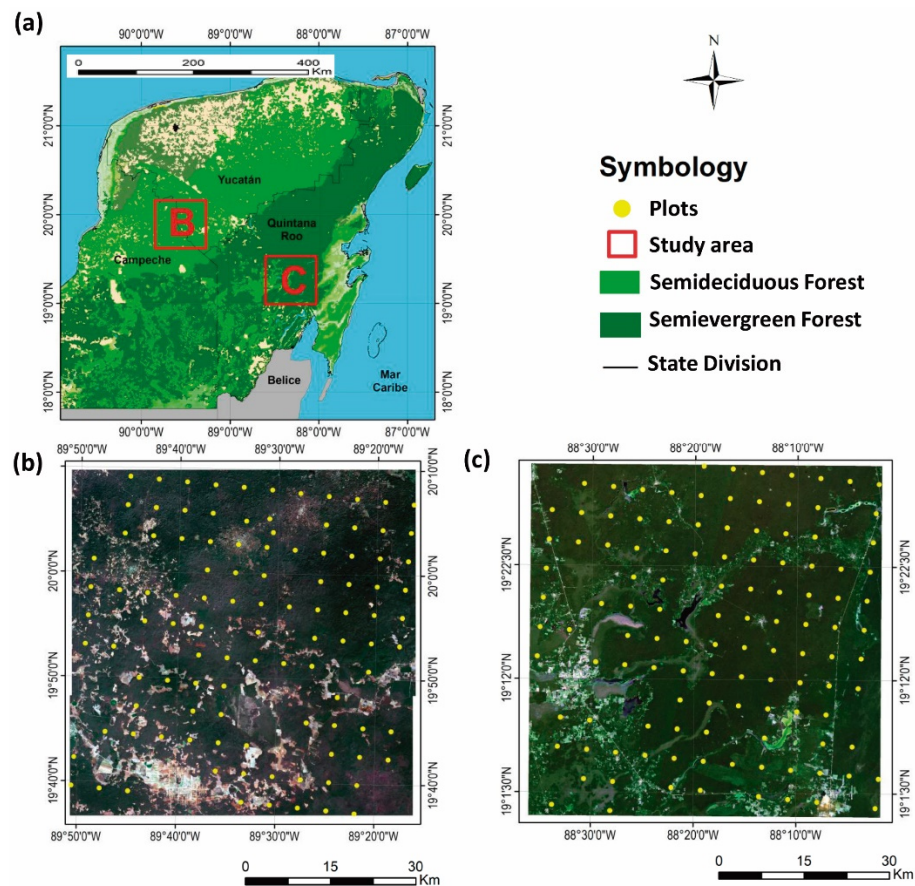


**Figure 1.** Location of the two study sites in the Yucatan peninsula (a). Distribution of the National Forest Inventory field plots in the tropical semi-deciduous forest (b) and the tropical semi-evergreen forest (c).

## 2.2. Field Data and Calculations of Tree Species Richness and Functional Diversity

We used data from the National Forest Inventory (INF) sampled between 2009 and 2014, with a total of 192 plots: 85 for Kaxil Kiuic and 107 for Felipe Carrillo Puerto. Each plot included four circular subplots of 400 m<sup>2</sup> distributed over an area of 1 ha, in which all trees  $\geq 7.5$  cm DBH (diameter at breast height, 1.3 m) were identified to species and measured (diameter and height). Species richness was determined as the number of tree species in each INF plot. Functional richness was calculated using six functional traits: wood density (dry weight divided by fresh volume), maximum height, leaf habit (deciduous vs. evergreen species), leaf dry matter content (dry weight divided by fresh weight), leaf area (leaf surface), and specific leaf area (surface area divided by dry weight). The attributes (value or modality) of each functional trait were obtained for most tree species sampled (82% and 71% of the species on average for Kaxil Kiuic and Felipe Carrillo Puerto, respectively). The attributes of each trait were obtained from local studies and online databases [42–46]. When it was not possible to obtain attributes at the species level, specimens were assigned the average for the genus or family or, as the last option, the average of the trait values for the species present in the sampling unit. Functional richness was estimated for each of the 192 plots using the FRic index proposed by Vileger et al. [13], calculated using the dbFD function of the FD package [47] in R. Traits were previously standardized so that all had a mean of zero and a variance of one [48]. Since not all traits were continuous variables—for example, leaf habit is a binary attribute (deciduous = 1; evergreen = 0)—Gower’s distance was used to estimate multivariate distances between species. In addition, the matrix of Gower’s distances was square root-transformed to avoid negative values. These distance data were subsequently subjected to a Principal Coordinate

Analysis (PCoA); the resulting PCoA axes were used as new compound functional traits for calculating functional richness [47].

### 2.3. Satellite Image Processing

Sentinel-2A-level sensor images collected between January and March 2018 were used. These images were previously orthorectified and radiometrically corrected. Of the thirteen spectral bands provided by Sentinel-2, only the four spectral bands with 10 m<sup>2</sup> spatial resolution were used to capture in more detail the spatial heterogeneity potentially related to species richness and functional richness in the study areas. The spectral bands considered in this study were the blue (458–523 nm), green (543–578 nm), red (650–680 nm), and near-infrared (NIR) (785–899 nm) bands.

Additionally, we calculated the Normalized Differential Vegetation Index (NDVI; [49]) using the Red and NIR bands in Equation (1) and the Soil-Adjusted Vegetation Index (SAVI), using Equation (2) with the Red and NIR bands as the parameters, as well as L—a soil adjustment factor with values ranging from 0 to 1. The SAVI index is an adjusted version of the NDVI that corrects the influence of soil brightness in areas with low vegetative coverage [50]. The formulas for vegetation indices are:

$$\text{NDVI} = (\text{NIR} - \text{Red}) / (\text{NIR} + \text{Red}) \quad (1)$$

$$\text{SAVI} = ((\text{NIR} - \text{Red}) / (\text{NIR} + \text{Red} + L)) \times (1 + L) \quad (2)$$

Eight second-order texture metrics were used to quantify the variability of neighboring pixel values [27]. Of these, three texture metrics quantify homogeneity (mean, correlation, and homogeneity), with high values of these variables indicating homogeneous zones. The other five texture metrics calculate heterogeneity (variance, contrast, entropy, dissimilarity, and second angular momentum), with high values in heterogeneous areas. Each of these metrics was calculated by applying a Gray Level Co-Occurrence Matrix (GLCM) with a window size of 9 × 9 pixels (0.81 ha), which is the area closest to the sample plot size (1.0 ha). Texture metrics were calculated in each spectral band and vegetation index in four orientations (0°, 45°, 90°, 135°); these were averaged to obtain a single texture value using the 'glcm' package [51] in R.

Due to the influence of topography on plant species richness and functional richness [11,52], the mean height above sea level of each sampling plot was calculated. For this purpose, digital elevation models (DEM) were acquired for each area studied. Each DEM was obtained from the ALOS PALSAR synthetic aperture radar. A resampling was necessary for the spatial resolution of DEMs (12.5 m) to match the spectral bands and vegetation indices (10 m).

Finally, we extracted the mean values of the pixels located within each 1-ha sampling unit of each spectral band and vegetation index. These values were also extracted from the texture metrics generated from spectral bands, vegetation indices, and DEMs. A total of 55 explanatory variables were extracted (Table 1). However, 27 variables with Pearson correlation values greater than 0.8 were removed from the analyses [53]. Therefore, only 28 variables were considered for estimating and mapping plant species richness and functional richness (dependent variables) in the study areas.

**Table 1.** Description of explanatory variables used to estimate species richness and functional diversity.

Type of Variable	Variable	DESCRIPTION
Sentinel-2	Blue	Reflectance of blue band
	Green	Reflectance of green band
	Red	Reflectance of red band
	NDVI	The normalized difference vegetation index [49]
	SAVI	The Soil-Adjusted Vegetation Index [50]
	Texture of Blue, Green, Red, NDVI and SAVI	The second-order texture measures used in this study are homogeneity (hom), contrast (cont), dissimilarity (dis), entropy (ent), angular second moment (asm), mean (mean), variance (var), and correlation (cor). See Haralick et al. [27] for details and formulas.
Topography	DEM	Digital elevation models (DEM) obtained from the ALOS PALSAR synthetic aperture radar.

#### 2.4. Estimating Species Richness and Functional Richness

Random Forest regression models were used to predict species richness and functional diversity from the explanatory variables obtained from spectral bands, vegetation indices, texture metrics, and topography. Models were constructed separately for species richness and functional diversity using the ModelMap package [54] in R. To this end, 70% of the plots (134 sampling units) were used for model calibration, and the remaining 30% (58 sampling units) were used as separate data for model validation. Model accuracy was assessed in terms of the coefficient of determination ( $R^2$ ), root mean square error (RMSE), and percentage of RMSE (%RMSE). Additionally, a spatial autocorrelation test was applied to the residuals of the calibrated models using Moran's I test. The importance of independent variables in predicting species richness and functional richness was determined using the percentage increase in the mean square error (% IncMSE) when the variable was removed from the model, so the higher the increase in the mean square error, the greater the importance of the variable in the prediction [54].

#### 2.5. Species Richness, Functional Diversity, and Their Associations

Using predictive models, we generated maps of the spatial distribution of species richness and functional diversity, as well as their respective maps of uncertainty in the study areas. Map quality was analyzed with uncertainty maps constructed by calculating the coefficient of variation (CV) for each pixel from the predictions of all the independent trees that composed the Random Forest model. All maps were obtained using the "model.mapmake" function from the ModelMap library [54] in R. Finally, a bivariate map was created by combining species richness and functional richness in a single map; this map shows the relationship between the number of species and functional richness for each pixel in the study areas.

Finally, the relationships between the eight most important variables included in the models and the species richness and functional richness were assessed using Pearson's correlation coefficient. Pearson's correlation coefficients between species richness and functional richness maps were calculated using all map pixels and field data.

### 3. Results

#### 3.1. Species Richness and Functional Diversity

A total of 16,650 trees belonging to 209 species were recorded on the 85 plots of the site located in the tropical semi-deciduous forest, while 17,493 trees belonging to 202 species were sampled on 107 plots in the tropical semi-evergreen forest. At the plot level, species richness and functional richness were higher in the semi-evergreen forest relative to the semi-deciduous forest, with mean species richness values of 32 and 21, respectively, and functional richness values of 47.2 and 17.3, respectively.

### 3.2. Performance of Models Predicting Species Richness and Functional Diversity

Models that predict species richness and functional richness using variables from satellite imagery (reflectance, vegetation indices, texture metrics, and DEM) are shown in Table 1. The percentages of variation in species richness and functional richness for the model using calibration data were  $R^2 = 0.32$  and  $0.36$ , respectively. The spatial autocorrelation of the residuals was not significant ( $p > 0.05$ ) for either model. Validation of the models with a separate dataset (Figure 2, Table 2) showed that the species richness model explained a greater percentage of the observed values (50%) compared with the functional richness model (44%). The relative RMSE values obtained were 25.4 and 48.8 for species richness and functional diversity, respectively (Figure 2).

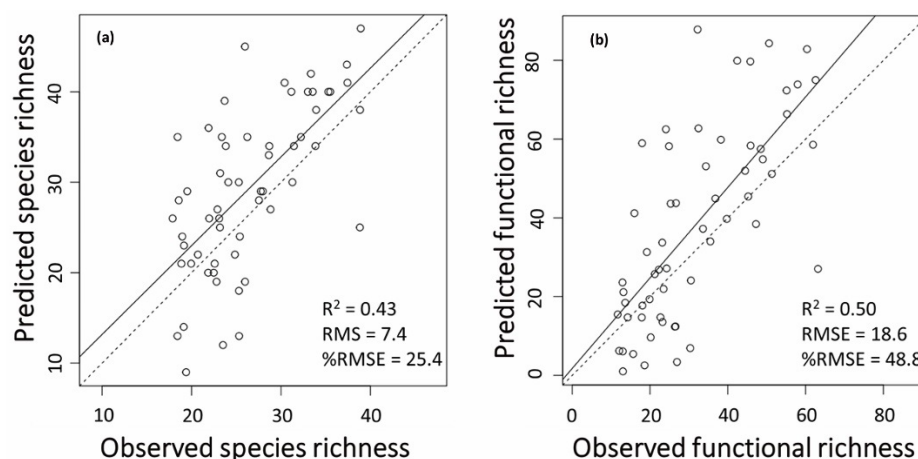


**Figure 2.** Comparison of observed versus predicted values for tree species richness (a) and functional richness (b). Dotted lines are 1:1 reference lines and solid lines are regression lines. The figure shows the coefficient of determination ( $R^2$ ), root mean square error (RMSE), and percentage of RMSE ( $\%RMSE$ ).

**Table 2.** Statistics of Random Forest models for estimating species richness and functional richness.

Variable	Type of Data	Number of Plots	$R^2$	RMSE	$\%RMSE$
Functional Richness	Calibration	174	0.36	21.0	65.5
Species Richness	Validation	58	0.50	18.6	48.8
Functional Richness	Calibration	174	0.32	9.0	33.9
Species Richness	Validation	58	0.44	7.4	25.4

The most important variables for predicting functional richness and tree species richness are shown in Figure 3. The most important predictors include texture metrics (Green Correlation, Red Correlation, Red Variance), as well as spectral bands (Green, Blue, NIR, Red). The eight most important variables in the models showed significant correlations with functional richness and tree species richness (Figure 3). Most texture metrics quantifying homogeneity (Green mean, Red correlation, SAVI correlation, Green correlation) were negatively related to functional richness and species richness (Green mean, Red mean, NIR homogeneity). On the other hand, the metrics quantifying heterogeneity were positively related to functional richness (Green dissimilarity, NIR contrast). However, one texture metric quantifying heterogeneity was negatively related species richness (Red variance). Regarding spectral bands, the green and blue bands were negatively related to functional richness and species richness, whereas the NIR and red bands were positively and negatively related to tree species richness, respectively.

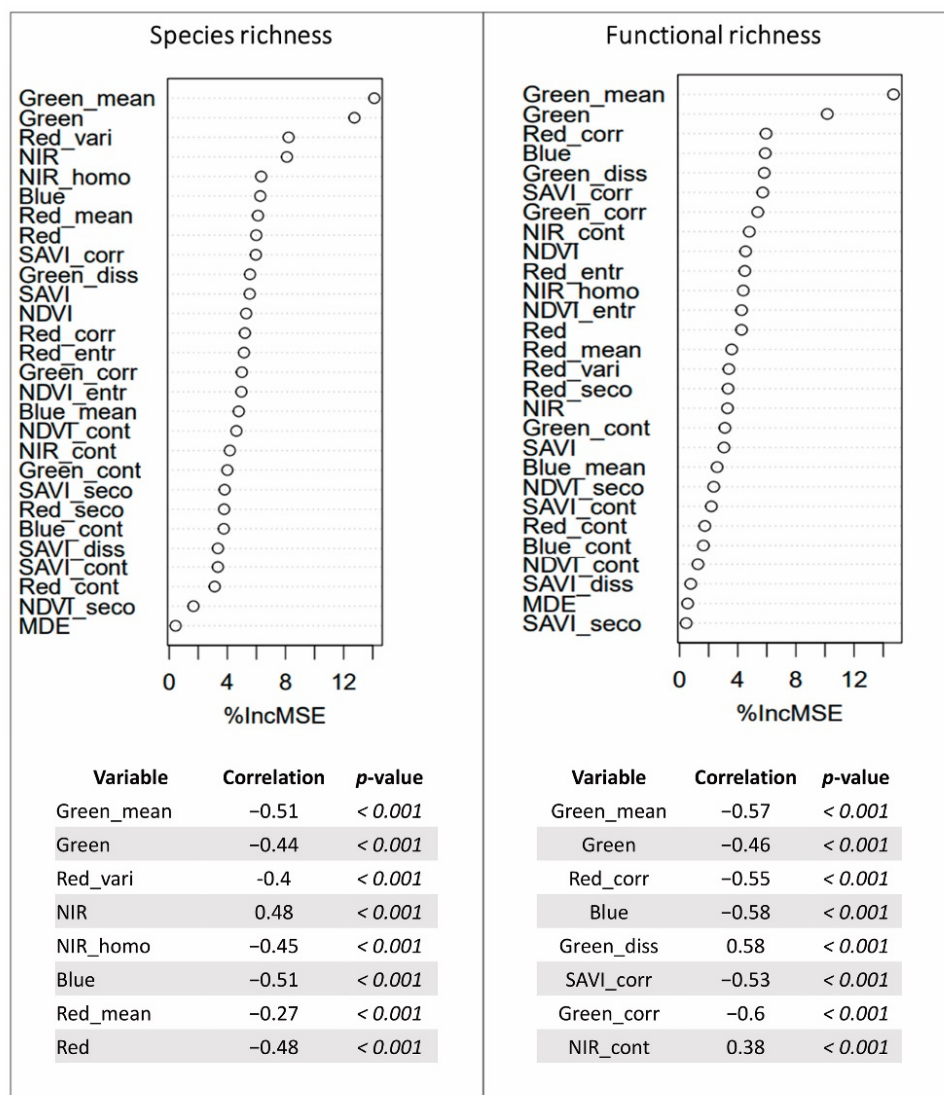


**Figure 3.** Classification of the importance of explanatory variables in estimating tree species richness and functional richness based on the percentage increase in mean square error (% incMSE) when the explanatory variable is removed. Pearson’s correlation coefficient to evaluate the type of relationship between the most important predictors and tree species richness and functional richness.

The species richness and functional richness maps for the two study sites were consistent with values observed in the field, i.e., species richness and functional diversity were higher in the semi-evergreen forest compared with the semi-deciduous forest. (28 and 39.34 vs. 19 and 25.5, respectively; Figure 4). On the other hand, uncertainty maps for species richness show that most of the surface area had values below 50% CV in the semi-deciduous forest and below 40% CV in the semi-evergreen forest (Figures 5a and 5b, respectively). For functional richness, uncertainty maps show that most of the surface area had values above 50% CV in the semi-deciduous forest and below 50% CV in the semi-evergreen forest (Figures 5c and 5d, respectively).



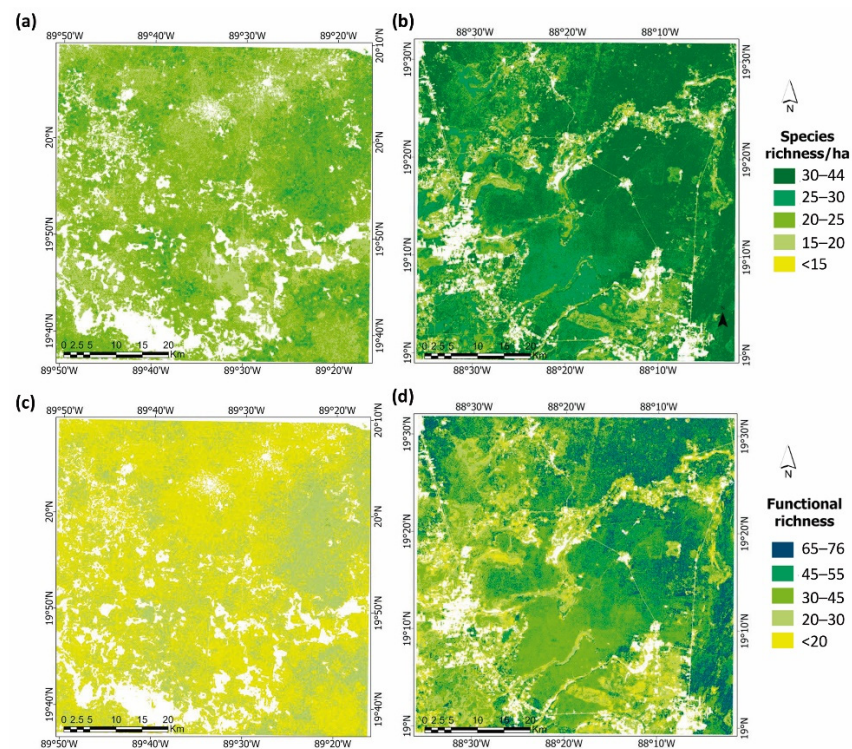


**Figure 4.** Maps of tree species richness and functional richness for the tropical semi-deciduous forest ((a) and (c), respectively) and the tropical semi-evergreen forest ((b) and (d), respectively). Blank areas correspond to non-forest cover (mostly cropland and human settlements).

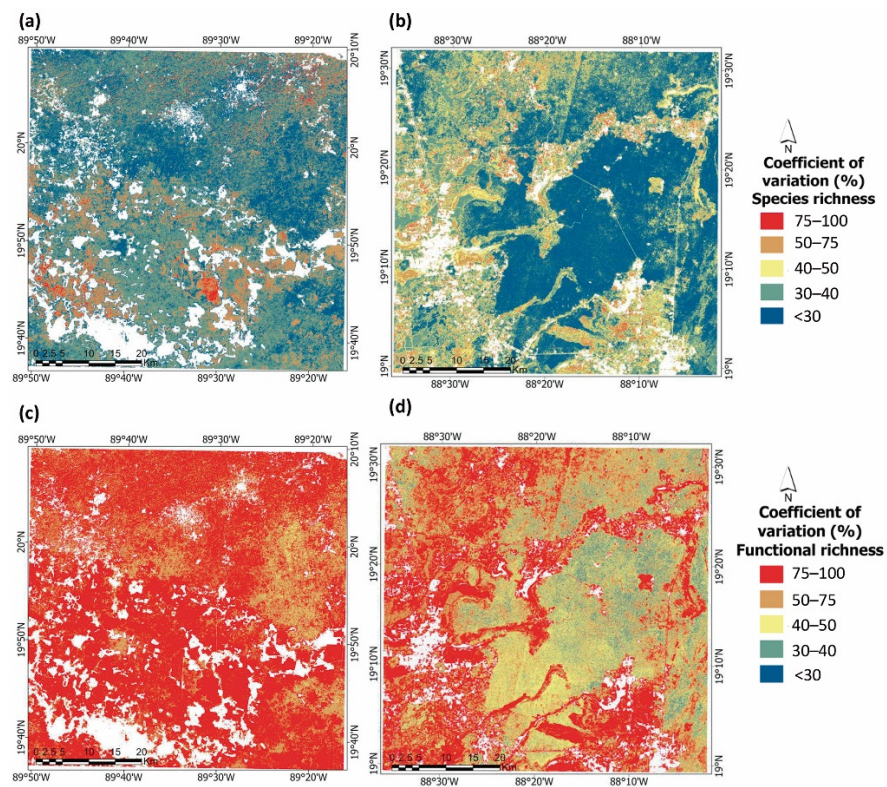


**Figure 5.** Uncertainty maps for tree species richness and functional richness for the tropical semi-deciduous forest ((a) and (b), respectively) and tropical semi-evergreen forest ((c) and (d), respectively). Blank areas correspond to non-forest cover (mostly cropland and human settlements).

### 3.3. Relationships between Species Richness and Functional Richness

Bivariate maps show the relationships between species richness and functional richness in the study area (Figure 6). It was observed that in the semi-evergreen forest, 44.9% of the surface area had high species richness and functional richness, while 44.0% showed low values of these attributes. On the other hand, in the semi-deciduous forest, 26.5% of the area showed high species richness and functional richness values, and 47.3% of the area showed low values of these attributes. Therefore, there is a direct relationship between species richness and functional richness in about 88.9% and 73.8% of the area covered with semi-evergreen forest and semi-deciduous forest, respectively.

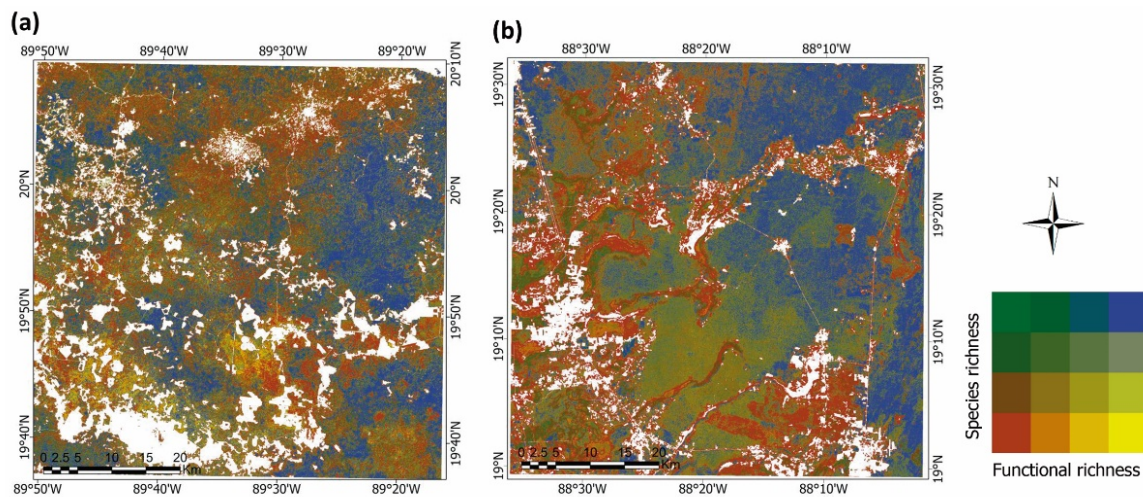


**Figure 6.** Maps showing the relationships between tree species richness and functional richness for the tropical semi-deciduous forest (a) and the tropical semi-evergreen forest (b).

The correlation between either tree species richness or functional richness and field data was high in the two forest types ( $r = 0.94$  and  $r = 0.96$  for the semi-deciduous forest and semi-evergreen forest, respectively). However, the semi-deciduous forest showed considerably lower correlations in the maps obtained ( $r = 0.59$ ). In contrast, the maps of tree species richness and functional richness for the semi-evergreen forest showed a very high correlation ( $r = 0.98$ ).

## 4. Discussion

### 4.1. Evaluation of Species Richness and Functional Richness Maps

This study demonstrated the potential of reflectance, vegetation indices, and texture metrics derived from Sentinel-2 imagery, in combination with field data for the number of species and functional traits, to model species richness and functional diversity in tropical dry forests. As far as we know, this is the first study modeling functional richness in this forest type. The models predicting the spatial distribution of the two vegetation attributes studied explained 32% and 36% of the variation for species richness and functional diversity, respectively, according to the models used with calibration data (Table 1). However, the coefficients of determination and the estimation error in the validation with a separate dataset show the predictive power of the models ( $R^2 = 0.44$  and %RMSE = 25.4 for species richness;  $R^2 = 0.50$  and %RMSE = 48.8, for functional diversity). Estimates of the spatial distribution of species richness showed patterns similar to those reported by Hernández-Stefanoni et al. [22] and Andres-Mauricio et al. [55], who constructed maps of tree species richness in the Yucatan Peninsula. However, this study showed a higher predictive power than the previous investigations, which yielded lower coefficients of determination and higher estimation errors.

Using Sentinel-2 imagery, the functional diversity maps obtained in this study can predict functional diversity for a larger geographic area than maps using hyperspectral imagery [17,30,32]. The predictive power of functional diversity using high-resolution

images in this study is consistent with the results reported by Ma et al. [8]. The authors generated functional diversity maps for different forest types in Europe using Sentinel-2 and reported validation coefficients of determination between 0.16 and 0.64 and a %RMSE between 27% and 43%. The results of this study, as well as those of Ma et al. [8], allow for the monitoring of functional diversity at regional scales and not only at the local level, as is the case with hyperspectral imagery. The uncertainty maps of tree species richness and functional richness showed the highest values in the semi-deciduous forest (Figures 4 and 5). Since top canopy trees are smaller in the semi-deciduous forest, a higher spatial resolution would be required to adequately characterize functional richness and diversity compared with the semi-evergreen forest.

A serious challenge when mapping functional diversity is the lack of field data representative of the functional traits of species in different ecosystems [33]. In other words, the quantity and quality of functional traits used for calculating functional richness indices are hugely important. In the present study, functional attributes were obtained from local studies and databases available online, in addition to assigning average values by plot to those species lacking measurements of these attributes. In fact, the uncertainty maps calculated to estimate species richness and functional diversity show higher coefficients of variation for functional richness. This may add a considerable error to functional richness values, affecting the associations with explanatory variables in Sentinel-2 imagery. An alternative to obtaining functional attributes without using field data is the use of high-resolution satellite images, as reported by Hauser et al. [56] who used Radiative Transfer Models. These models could be a starting point for estimating functional diversity in the absence of field data.

Texture metrics, vegetation indices, and spectral bands proved to be suitable predictors of tree species richness and functional richness in the forests studied. Texture metrics quantifying spectral homogeneity were negatively related to species richness and functional richness. This finding is consistent with the spectral variation hypothesis [26]. It is widely recognized that species richness increases with habitat heterogeneity as heterogeneous habitats provide more niches than do homogeneous habitats [26,57,58]. On the other hand, this suggests that low functional richness translates into little variability in characteristics such as crown architecture, leaf area index, specific leaf area, or tree height (convergence of traits) [59], probably as a result of poorly contrasting environmental conditions, which would favor the dominance of a few species with similar ecological strategies and functional traits. That is, the negative relationship between spectral homogeneity and species richness may be due to areas with climatic, topographic, and edaphic characteristics with insufficient spatial variations to produce species turnover, which may also be dominated by similar functional attributes, thus reflecting low functional richness. Examples are species with a deciduous or perennial canopy, depending on the prevailing environmental conditions, leading to a low mixture of spectral signatures by species (spectral homogeneity).

On the other hand, species richness increases with habitat heterogeneity because local environmental heterogeneity promotes the coexistence between species by providing different microhabitats and, thus, a higher number of available ecological niches [59,60]. The same argumentation explains the positive relationships between functional richness and some heterogeneity metrics. Some areas possibly have an unequal distribution of water, nutrients, and light that results in a mixture of species with deciduous or evergreen canopies and different leaf characteristics; this would reflect a high spectral variability in imagery and high functional diversity levels due to differences in the ecological strategies of species. These results are consistent with the findings reported by Schweiger et al. [7], who observed that functionally different species produced different spectral signatures. These results highlight the importance of using texture metrics in studies aiming to evaluate functional richness in plant communities through remote sensing.

The negative correlations of species richness and functional richness with the blue and red spectral bands may be attributed to the fact that a higher density of healthy or “vigorous” vegetation would show a higher absorption in the visible spectrum [24] because

of the higher absorption by leaf pigments in this region. Finally, the positive correlation between species richness and the near-infrared band (NIR) is due to the high reflectivity of the NIR in healthy vegetation [24]. This behavior is related to leaf pigments, the mesophyll structure, and the amount of water stored in the latter [24].

#### 4.2. Relationships between Tree Species Richness and Functional Richness

Conservation and restoration activities aim to preserve biodiversity and ecosystem services [61]. To this end, it is necessary to obtain accurate regional information not only on the spatial distribution of plant species richness and functional richness [16,62] but also on the spatial distribution of the relationships between both variables [63]. The results of the present study indicate that species richness was positively related to functional diversity in almost 75% of the area covered with tropical semi-deciduous forest and in almost 90% of the area of tropical semi-evergreen forest. These findings are consistent with previous studies reporting positive associations between plant species richness and functional richness [36,62]. These results may support the planning and management of activities that simultaneously promote biodiversity conservation and the provision of ecosystem services, such as primary productivity and mitigation of global climate change through atmospheric carbon uptake and storage in terrestrial ecosystems. For instance, areas with high species richness and functional richness are highly relevant for biodiversity conservation and the provision of ecosystem services, while areas with low values of both variables may require restoration plans and actions. In this sense, it is remarkable that the semi-evergreen forest landscape showed a higher percentage of its area with high values of both variables than did the semi-deciduous forest landscape (44.9% vs. 26.5%), while the percentage with low values of both variables showed the opposite pattern (44% vs. 47.3%, respectively). These results suggest a greater adverse impact of anthropogenic activities on the semi-deciduous forest than on the semi-evergreen forest landscape. However, the area currently devoted to non-forest land use is smaller in the former than in the latter. The largest area with low taxonomic and functional richness in the semi-deciduous tropical forest is likely because this landscape underwent longer and more widespread anthropogenic uses throughout history than the semi-evergreen forest. On the other hand, the smaller percentage of area with a positive relationship between taxonomic richness and functional richness in the semi-deciduous forest, compared with the semi-evergreen forest landscape, may be partly due to the greater uncertainty in the estimates of both variables in the former (Figure 6).

## 5. Conclusions

This study demonstrated the potential of Sentinel-2 imagery, in combination with field data on the number of species and functional traits, to model species richness and functional diversity in tropical dry forests. Models for estimating these variables have an acceptable predictive power ( $R^2 = 0.44$  and %RMSE = 25.4 for species richness;  $R^2 = 0.50$  and %RMSE = 48.8 for functional diversity). Texture metrics, vegetation indices, and spectral bands proved to be suitable predictors of tree species richness and functional richness in the forests studied. Texture metrics were among the most important variables for estimating these two variables. This result demonstrates the importance of using texture metrics not only for estimating species richness but also in studies assessing functional richness in plant communities with remote sensing tools.

Finally, maps were constructed with the relationships between plant species richness and functional richness in two tropical dry forests of the Yucatan Peninsula. A positive correlation was found in 88.9% and 73.8% of the area covered with semi-deciduous and semi-evergreen forests, respectively, with high values of both variables in 44.9% and 26.5% of the areas, respectively. Preserving these areas is highly relevant for biodiversity conservation, and the provision of ecosystem services and climate change mitigation, while areas with low values of both variables (44% and 47.3%, respectively) probably require restoration plans and actions.

**Author Contributions:** V.A.P.-L. and J.L.H.-S. conceived the research and designed the experiments; V.A.P.-L., J.M.D. and J.L.H.-S. wrote the first draft of the manuscript; V.A.P.-L. processed the field data; V.A.P.-L. processed Sentinel-2 imagery; and V.A.P.-L. and J.L.H.-S. performed the statistical analysis. V.A.P.-L., J.M.D., C.R.-G., L.S.-V., C.A.P.-Q. and J.L.H.-S. discussed the results, commented on the manuscript, shared equally in the editing of the manuscript, and approved the final version of the paper. All authors have read and agreed to the published version of the manuscript.

**Funding:** The study was financially supported by CICY and Ecometrica LTD and the United Kingdom Space Agency as part of the project Forests 2020. This study is part of the first author's MSc. dissertation which was supported by a grant from CONACYT.

**Data Availability Statement:** The Sentinel-2 data can be accessed at (<https://scihub.copernicus.eu/>, accessed on 1 June 2021). Data from the Mexican National Forest Inventory can be obtained by request from CONAFOR (Comisión Nacional Forestal, <https://www.gob.mx/conafor>, accessed on 1 June 2021).

**Acknowledgments:** We thank the ejidos of Xkobehnaltún, Xuul, Yaxhachén, and Felipe Carrillo Puerto for allowing us to work in their lands and for their assistance with fieldwork. James Callaghan and Reserva Biocultural Kaxil Kiuic provided logistic support. María. E Sanchez-Salazar translated the first draft of the manuscript into English. We also thank the Mexican National Forestry Commission (CONAFOR) for kindly providing forest inventory data.

**Conflicts of Interest:** The authors declare no conflict of interest.

## References

1. Powers, J.S.; Feng, X.; Sanchez-Azofeifa, A.; Medvigy, D. Focus on tropical dry forest ecosystems and ecosystem services in the face of global change. *Environ. Res. Lett.* **2018**, *13*, 090201. [[CrossRef](#)]
2. Portillo-Quintero, C.A.; Sánchez-Azofeifa, G.A. Extent and conservation of tropical dry forests in the Americas. *Biol. Conserv.* **2010**, *143*, 144–155. [[CrossRef](#)]
3. Portillo-Quintero, C.; Sanchez-Azofeifa, A.; Calvo-Alvarado, J.; Quesada, M.; do Espirito Santo, M.M. The role of tropical dry forests for biodiversity, carbon and water conservation in the neotropics: Lessons learned and opportunities for its sustainable management. *Reg. Environ. Chang.* **2015**, *15*, 1039–1049. [[CrossRef](#)]
4. Van der Plas, F. Biodiversity and ecosystem functioning in naturally assembled communities. *Biol. Rev.* **2019**, *94*, 1220–1245. [[CrossRef](#)]
5. Stuart-Smith, R.D.; Bates, A.E.; Lefcheck, J.S.; Duffy, J.E.; Baker, S.C.; Thomson, R.J.; Stuart-Smith, J.F.; Hill, N.A.; Kininmonth, S.J.; Airoidi, L.; et al. Integrating abundance and functional traits reveals new global hotspots of fish diversity. *Nature* **2013**, *501*, 539–542. [[CrossRef](#)]
6. Díaz, S.; Cabido, M. Vive la différence: Plant functional diversity matters to ecosystem processes. *Trends Ecol. Evol.* **2002**, *16*, 646–655. [[CrossRef](#)]
7. Schweiger, A.K.; Cavender-Bares, J.; Townsend, P.A.; Hobbie, S.E.; Madritch, M.D.; Wang, R.; Tilman, D.; Gamon, J.A. Plant spectral diversity integrates functional and phylogenetic components of biodiversity and predicts ecosystem function. *Nat. Ecol. Evol.* **2018**, *2*, 976–982. [[CrossRef](#)]
8. Ma, X.; Mahecha, M.D.; Migliavacca, M.; Van Der Plas, F.; Benavides, R.; Ratcliffe, S.; Kattge, J.; Richter, R.; Musavi, T.; Baeten, L.; et al. Inferring plant functional diversity from space: The potential of Sentinel-2. *Remote Sens. Environ.* **2019**, *233*, 111368. [[CrossRef](#)]
9. Correa, J.B.; Torres, J.P. Functional diversity: A key aspect in the provision of ecosystem services. *Rev. Colomb. Cienc. Anim.-RECIA* **2016**, *8*, 94–111. [[CrossRef](#)]
10. Violle, C.; Navas, M.-L.; Vile, D.; Kazakou, E.; Fortunel, C.; Hummel, I.; Garnier, E. Let the concept of trait be functional! *Oikos* **2007**, *116*, 882–892. [[CrossRef](#)]
11. Sanaphre-Villanueva, L.; Dupuy, J.M.; Andrade, J.L.; Reyes-García, C.; Paz, H.; Jackson, P.C. Functional diversity of small and large trees along secondary succession in a tropical dry forest. *Forests* **2016**, *7*, 163. [[CrossRef](#)]
12. Mason, N.W.; Mouillot, D.; Lee, W.G.; Wilson, J.B. Functional richness, functional evenness and functional divergence: The primary components of functional diversity. *Oikos* **2005**, *111*, 112–118. [[CrossRef](#)]
13. Villéger, S.; Mason, N.W.; Mouillot, D. New multidimensional functional diversity indices for a multifaceted framework in functional ecology. *Ecology* **2008**, *89*, 2290–2301. [[CrossRef](#)]
14. Mouchet, M.A.; Villéger, S.; Mason, N.W.; Mouillot, D. Functional diversity measures: An overview of their redundancy and their ability to discriminate community assembly rules. *Funct. Ecol.* **2010**, *24*, 867–876. [[CrossRef](#)]
15. Mouillot, D.; Villéger, S.; Scherer-Lorenzen, M.; Mason, N.W. Functional structure of biological communities predicts ecosystem multifunctionality. *PLoS ONE* **2011**, *6*, e17476. [[CrossRef](#)] [[PubMed](#)]
16. Huang, X.; Su, J.; Li, S.; Liu, W.; Lang, X. Functional diversity drives ecosystem multifunctionality in a *Pinus yunnanensis* natural secondary forest. *Sci. Rep.* **2019**, *9*, 6979. [[CrossRef](#)]

17. Durán, S.M.; Martin, R.E.; Díaz, S.; Maitner, B.S.; Malhi, Y.; Salinas, N.; Shenkin, A.; Silman, M.R.; Wiczynski, D.J.; Asner, G.P.; et al. Informing trait-based ecology by assessing remotely sensed functional diversity across a broad tropical temperature gradient. *Sci. Adv.* **2019**, *5*, eaaw8114. [[CrossRef](#)]
18. Beer, C.; Reichstein, M.; Tomelleri, E.; Ciais, P.; Jung, M.; Carvalhais, N.; Rödenbeck, C.; Arain, M.A.; Baldocchi, D.; Bonan, G.B.; et al. Terrestrial gross carbon dioxide uptake: Global distribution and covariation with climate. *Science* **2010**, *329*, 834–838. [[CrossRef](#)]
19. Wang, R.; Gamon, J.A. Remote sensing of terrestrial plant biodiversity. *Remote Sens. Environ.* **2019**, *231*, 111218. [[CrossRef](#)]
20. Kier, G.; Mutke, J.; Dinerstein, E.; Ricketts, T.H.; Küper, W.; Kreft, H.; Barthlott, W. Global patterns of plant diversity and floristic knowledge. *J. Biogeogr.* **2005**, *32*, 1107–1116. [[CrossRef](#)]
21. Kreft, H.; Jetz, W. Global patterns and determinants of vascular plant diversity. *Proc. Natl. Acad. Sci. USA* **2007**, *104*, 5925–5930. [[CrossRef](#)] [[PubMed](#)]
22. Hernández-Stefanoni, J.L.; Castillo-Santiago, M.Á.; Andres-Mauricio, J.; Portillo-Quintero, C.A.; Tun-Dzul, F.; Dupuy, J.M. Carbon Stocks, Species Diversity and Their Spatial Relationships in the Yucatán Peninsula, Mexico. *Remote Sens.* **2021**, *13*, 3179. [[CrossRef](#)]
23. George-Chacon, S.P.; Dupuy, J.M.; Peduzzi, A.; Hernandez-Stefanoni, J.L. Combining high resolution satellite imagery and lidar data to model woody species diversity of tropical dry forests. *Ecol. Indic.* **2019**, *101*, 975–984. [[CrossRef](#)]
24. Vieira, I.C.G.; de Almeida, A.S.; Davidson, E.A.; Stone, T.A.; de Carvalho, C.J.R.; Guerrero, J.B. Classifying successional forests using Landsat spectral properties and ecological characteristics in eastern Amazonia. *Remote Sens. Environ.* **2003**, *87*, 470–481. [[CrossRef](#)]
25. Oehri, J.; Schmid, B.; Schaepman-Strub, G.; Niklaus, P.A. Biodiversity promotes primary productivity and growing season lengthening at the landscape scale. *Proc. Natl. Acad. Sci. USA* **2017**, *114*, 10160–10165. [[CrossRef](#)]
26. Rocchini, D.; Balkenhol, N.; Carter, G.A.; Foody, G.M.; Gillespie, T.W.; He, K.S.; Kark, S.; Levin, N.; Lucas, K.; Luoto, M.; et al. Remotely sensed spectral heterogeneity as a proxy of species diversity: Recent advances and open challenges. *Ecol. Inform.* **2010**, *5*, 318–329. [[CrossRef](#)]
27. Haralick, R.M.; Shanmugam, K.; Dinstein, I.H. Textural features for image classification. *IEEE Trans. Syst. Man Cybern.* **1973**, *SMC-3*, 610–621. [[CrossRef](#)]
28. Moreno-Martínez, Á.; Camps-Valls, G.; Kattge, J.; Robinson, N.; Reichstein, M.; van Bodegom, P.; Kramer, K.; Cornelissen, J.H.C.; Reich, P.; Bahn, M.; et al. A methodology to derive global maps of leaf traits using remote sensing and climate data. *Remote Sens. Environ.* **2018**, *218*, 69–88. [[CrossRef](#)]
29. Cavender-Bares, J.; Meireles, J.E.; Couture, J.J.; Kaproth, M.A.; Kingdon, C.C.; Singh, A.; Serbin, S.P.; Center, A.; Zuniga, E.; Pilz, G.; et al. Associations of leaf spectra with genetic and phylogenetic variation in oaks: Prospects for remote detection of biodiversity. *Remote Sens.* **2016**, *8*, 221. [[CrossRef](#)]
30. Zheng, Z.; Zeng, Y.; Schneider, F.D.; Zhao, Y.; Zhao, D.; Schmid, B.; Schaepman, M.E.; Morsdorf, F. Mapping functional diversity using individual tree-based morphological and physiological traits in a subtropical forest. *Remote Sens. Environ.* **2021**, *252*, 112170. [[CrossRef](#)]
31. Asner, G.P.; Martin, R.E.; Knapp, D.E.; Tupayachi, R.; Anderson, C.B.; Sinca, F.; Vaughn, N.R.; Llactayo, W. Airborne laser-guided imaging spectroscopy to map forest trait diversity and guide conservation. *Science* **2017**, *355*, 385–389. [[CrossRef](#)] [[PubMed](#)]
32. Schneider, F.D.; Morsdorf, F.; Schmid, B.; Petchey, O.L.; Hueni, A.; Schimel, D.S.; Schaepman, M.E. Mapping functional diversity from remotely sensed morphological and physiological forest traits. *Nat. Commun.* **2017**, *8*, 1441. [[CrossRef](#)] [[PubMed](#)]
33. Aguirre-Gutiérrez, J.; Rifai, S.; Shenkin, A.; Oliveras, I.; Bentley, L.P.; Svátek, M.; Girardin, C.A.; Both, S.; Riutta, T.; Berenguer, E.; et al. Pan-tropical modelling of canopy functional traits using Sentinel-2 remote sensing data. *Remote Sens. Environ.* **2021**, *252*, 112122. [[CrossRef](#)]
34. Wallis, C.I.; Homeier, J.; Peña, J.; Brandl, R.; Farwig, N.; Bendix, J. Modeling tropical montane forest biomass, productivity and canopy traits with multispectral remote sensing data. *Remote Sens. Environ.* **2019**, *225*, 77–92. [[CrossRef](#)]
35. Fischer, R.; Knapp, N.; Bohn, F.; Shugart, H.H.; Huth, A. The relevance of forest structure for biomass and productivity in temperate forests: New perspectives for remote sensing. *Surv. Geophys.* **2019**, *40*, 709–734. [[CrossRef](#)]
36. Karadimou, E.K.; Kallimanis, A.S.; Tsiripidis, I.; Dimopoulos, P. Functional diversity exhibits a diverse relationship with area, even a decreasing one. *Sci. Rep.* **2016**, *6*, 35420. [[CrossRef](#)] [[PubMed](#)]
37. Roscher, C.; Schumacher, J.; Gerighausen, U.; Schmid, B. Different assembly processes drive shifts in species and functional composition in experimental grasslands varying in sown diversity and community history. *PLoS ONE* **2014**, *9*, e101928. [[CrossRef](#)]
38. Pakeman, R.J. Functional diversity indices reveal the impacts of land use intensification on plant community assembly. *J. Ecol.* **2011**, *99*, 1143–1151. [[CrossRef](#)]
39. Miranda, F.; Hernández, X.E. *Los Tipos de Vegetación de México y su Clasificación*; Escuela Nacional de Agricultura, Colegio de Postgraduados: Texcoco, Mexico, 1963; p. 151.
40. Orellana, R.; Islebe, G.A.; González-Iturbe, J.A. *Presente, Pasado y Futuro de los Climas de la Península de Yucatán. En Naturaleza y Sociedad en el área Maya*; Marín, P.C.-G., Saavedra, A.L., Eds.; Academia Mexicana de Ciencias, Centro de Investigación Científica de Yucatán: Mérida, México, 2003; pp. 37–52.
41. Hernández-Stefanoni, J.L.; Dupuy, J.M.; Jhonson, K.J.; Birdsey, R.; Tun-Dzul, F.; Peduzzi, A.; Camal-Sosa, J.P.; Sánchez-Santos, G.; López-Merlín, D. Improving Species Diversity and Biomass Estimates of Tropical Dry Forest Using Airborne LiDAR. *Remote Sens.* **2014**, *6*, 4741–4763. [[CrossRef](#)]

42. Huechacona-Ruiz, A.H.; Dupuy, J.M.; Schwartz, N.B.; Powers, J.S.; Reyes-García, C.; Tun-Dzul, F.; Hernández-Stefanoni, J.L. Mapping tree species deciduousness of tropical dry forests combining reflectance, spectral unmixing, and texture data from high-resolution imagery. *Forests* **2020**, *11*, 1234. [[CrossRef](#)]
43. Hernández-Stefanoni, J.L.; Castillo-Santiago, M.; Mas, J.F.; Wheeler, C.E.; Andres-Mauricio, J.; Tun-Dzul, F.; George-Chacón, S.P.; Reyes-Palomeque, G.; Castellanos-Basto, B.; Vaca, R.; et al. Improving aboveground biomass maps of tropical dry forests by integrating LiDAR, ALOS PALSAR, climate and field data. *Carbon Balance Manag.* **2020**, *15*, 15. [[CrossRef](#)] [[PubMed](#)]
44. Kattge, J.; Bönisch, G.; Díaz, S.; Lavorel, S.; Prentice, I.C.; Leadley, P.; Tautenhahn, S.; Werner, G.D.A.; Aakala, T.; Abedi, M.; et al. TRY plant trait database—Enhanced coverage and open access. *Glob. Chang. Biol.* **2020**, *26*, 119–188. [[CrossRef](#)] [[PubMed](#)]
45. Sanaphre-Villanueva, L.; Dupuy, J.M.; Andrade, J.L.; Reyes-García, C.; Jackson, P.C.; Paz, H. Patterns of plant functional variation and specialization along secondary succession and topography in a tropical dry forest. *Environ. Res. Lett.* **2017**, *12*, 055004. [[CrossRef](#)]
46. Letcher, S.G.; Lasky, J.R.; Chazdon, R.L.; Norden, N.; Wright, S.J.; Meave, J.A.; Pérez-García, E.A.; Muñoz, R.; Romero-Pérez, E.; Andrade, A.; et al. Environmental gradients and the evolution of successional habitat specialization: A test case with 14 Neotropical forest sites. *J. Ecol.* **2015**, *103*, 1276–1290. [[CrossRef](#)]
47. Laliberté, E.; Legendre, P. A distance-based framework for measuring functional diversity from multiple traits. *Ecology* **2010**, *91*, 299–305. [[CrossRef](#)]
48. Swenson, N.G.; Weiser, M.D.; Mao, L.; Araújo, M.B.; Diniz-Filho, J.A.F.; Kollmann, J.; Nogués-Bravo, D.; Normand, S.; Rodríguez, M.A.; García-Valdés, R.; et al. Phylogeny and the prediction of tree functional diversity across novel continental settings. *Glob. Ecol. Biogeogr.* **2017**, *26*, 553–562. [[CrossRef](#)]
49. Rousel, J.; Haas, R.; Schell, J.; Deering, D. Monitoring vegetation systems in the great plains with ERTS. In Proceedings of the Third Earth Resources Technology Satellite—1 Symposium, NASA SP-351, Washington, DC, USA, 10–15 December 1974; pp. 309–317.
50. Huete, A.R. A soil-adjusted vegetation index (SAVI). *Remote Sens. Environ.* **1988**, *25*, 295–309. [[CrossRef](#)]
51. Zvovoff, A. Package ‘glcm’. Calculate Textures from Grey-Level Co-Occurrence Matrices (GLCMs). Available online: <https://cran.r-project.org/web/packages/glcm/index.html> (accessed on 25 October 2022).
52. Dupuy, J.M.; Hernandez-Stefanoni, J.L.; Hernández-Juárez, R.A.; Tetetla-Rangel, E.; López-Martínez, J.O.; Leyequién-Abarca, E.; Tun-Dzul, F.J.; May-Pat, F. Patterns and correlates of tropical dry forest structure and composition in a highly replicated chronosequence in Yucatan, Mexico. *Biotropica* **2012**, *44*, 151–162. [[CrossRef](#)]
53. Liaw, A.; Wiener, M. Classification and regression by randomForest. *R News* **2002**, *2*, 18–22.
54. Freeman, E.A.; Frescino, T.S.; Moisen, G.G. ModelMap: An R Package for Model Creation and Map Production. Available online: <https://cran.r-project.org/web/packages/ModelMap/vignettes/VModelMap.pdf> (accessed on 18 October 2022).
55. Andres-Mauricio, J.; Valdez-Lazalde, J.R.; George-Chacón, S.P.; Hernández-Stefanoni, J.L. Mapping structural attributes of tropical dry forests by combining Synthetic Aperture Radar and high-resolution satellite imagery data. *Appl. Veg. Sci.* **2021**, *24*, e12580. [[CrossRef](#)]
56. Hauser, L.T.; Féret, J.-B.; Binh, N.A.; van der Windt, N.; Sil, F.; Timmermans, J.; Soudzilovskaia, N.A.; van Bodegom, P.M. Towards scalable estimation of plant functional diversity from Sentinel-2: In-situ validation in a heterogeneous (semi-)natural landscape. *Remote Sens. Environ.* **2021**, *262*, 112505. [[CrossRef](#)]
57. Warren, S.D.; Alt, M.; Olson, K.D.; Irl, S.D.; Steinbauer, M.J.; Jentsch, A. The relationship between the spectral diversity of satellite imagery, habitat heterogeneity, and plant species richness. *Ecol. Inform.* **2014**, *24*, 160–168. [[CrossRef](#)]
58. Stein, A.; Gerstner, K.; Kreft, H. Environmental heterogeneity as a universal driver of species richness across taxa, biomes and spatial scales. *Ecol. Lett.* **2014**, *17*, 866–880. [[CrossRef](#)] [[PubMed](#)]
59. Bergholz, K.; May, F.; Giladi, I.; Ristow, M.; Ziv, Y.; Jeltsch, F. Environmental heterogeneity drives fine-scale species assembly and functional diversity of annual plants in a semi-arid environment. *Perspect. Plant Ecol. Evol. Syst.* **2017**, *24*, 138–146. [[CrossRef](#)]
60. Schmidtlein, S.; Fassnacht, F.E. The spectral variability hypothesis does not hold across landscapes. *Remote Sens. Environ.* **2017**, *192*, 114–125. [[CrossRef](#)]
61. Cadotte, M.W.; Carscadden, K.; Mirotchnick, N. Beyond species: Functional diversity and the maintenance of ecological processes and services. *J. Appl. Ecol.* **2011**, *48*, 1079–1087. [[CrossRef](#)]
62. Conroy, M.J.; Noon, B.R. Mapping of species richness for conservation of biological diversity: Conceptual and methodological issues. *Ecol. Appl.* **1996**, *6*, 763–773. [[CrossRef](#)]
63. Suárez-Castro, A.F.; Raymundo, M.; Bimler, M.; Mayfield, M.M. Using multi-scale spatially explicit frameworks to understand the relationship between functional diversity and species richness. *Ecography* **2022**, *22*, e05844. [[CrossRef](#)]